Young's Double-Slit Interference Observation of Hot Electrons in Semiconductors

Kazuhito Furuya,[1,2,3,*] Yasunori Ninomiya,[1] Nobuya Machida,[1,3] and Yasuyuki Miyamoto[1,3]

[1]*Graduate School of Science and Engineering, Tokyo Institute of Technology, 2-12-1 Ookayama, Meguro-ku, Tokyo 152-8552, Japan*

[2]*Research Center of Quantum Effect Electronics, Tokyo Institute of Technology, 2-12-1 Ookayama, Meguro-ku, Tokyo 152-8552, Japan*

[3]*CREST, Japan Science and Technology Corporation, 4-1-8 Honmachi, Kawaguchi-shi, Saitama 332-0012, Japan*

(Received 2 May 2003; published 19 November 2003)

We have carried out Young's double-slit experiment for the hot-electron wave in man-made semiconductor structures with a 25-nm-space double slit in an InP layer buried within GaInAs, a 190-nm-thick GaInAsP hot-electron wave propagation layer, and a collector array of 80 nm pitch. At 4.2 K, dependences of the collector current on the magnetic field were measured and found to agree clearly with the double-slit interference theory. The present results show evidence for the wave front spread of hot electrons using the three-dimensional state in materials, for the first time, and the possibility of using top-down fabrication techniques to achieve quantum wave front control in materials.

DOI: 10.1103/PhysRevLett.91.216803 PACS numbers: 73.23.Ad

Quantum wave phenomena of electrons in semiconductors could give rise to future electron devices and are very attractive [1,2]. Wave behaviors of electrons close to equilibrium at low temperature have been intensively studied. In particular, interferences of the two-dimensional electron gas (2DEG) have been definitively demonstrated [3–5]. Employing the injector/collector composed of quantum point contacts (QPCs) prepared by the split-gate technique [6] and magnetic field steering, diffraction patterns caused by QPC apertures [7], and interference patterns caused by impurity ions [8] were clearly observed.

On the other hand, devices based on ballistic hot electrons, or nonequilibrium electrons, have been proposed [9,10]. The use of ballistic hot electrons has effectively sped up heterojunction bipolar transistors [11]. Characteristics of ballistic hot electrons have been studied employing the ballistic electron emission microscope or the hot-electron tunnel emitter combined with the double-barrier resonant tunneling structure [12] or electroluminescence [13]. Coherent wave properties of ballistic hot electrons have been revealed by observations of the resonant tunneling [12] and Wannier-Stark states in the superlattice [14].

Among coherent wave properties, wave fronts of ballistic hot electrons in semiconductors have been received much attention [15]. In transmission electron microscopy, the wave front of the electron beam is modulated by a crystal lattice, which causes diffraction. The diffraction pattern corresponds to the Fourier transform of the potential distribution of the crystal lattice. Electron holography is another example of wave front manipulation [16]. So far, the electron-wave Fourier transform and electron holography take place only in a vacuum. Once the manipulation of the wave front of the ballistic hot electron is achieved in materials, novel devices could be created. However, wave front manipulation in materials is not easy. Limited wave front spreads, ultrafine structures required for manipulation, and ultrahigh resolution required for observation are hurdles to overcome.

We proposed a double-slit interference experiment on the hot electron [17] and attempted interference observation, for the first time, by magnetic field steering [18]. The collector current was modulated by 1% and showed a clear minimum at zero magnetic field, in agreement with the theory. The first trial inspired us to further confirm the observation by enhancing interference contrast. To further enhance the contrast, the double-slit space [19] and the collector array pitch [20] were reduced. Isolation of collectors was accomplished by introducing heterojunctions [21].

In this Letter, we report the clear observation of the double-slit interference of the hot electron in devices fabricated using the above-mentioned techniques. The present observation is different from previous works on 2DEG with respect to the electron state and the structure causing the interference. That is, here, the electron wave propagates as a three-dimensional and nonequilibrium electron in an intrinsic semiconductor instead of the two-dimensional and near-equilibrium electron in the modulation-doped structure. The interference is caused by the nanometer-size double slit prepared by top-down fabrication processes, instead of the constriction due to the split-gate or impurity atoms included unintentionally.

A band profile and a cross section of the fabricated devices are shown in Fig. 1. The emitter consists of an emitter electrode, a grading composition layer, a barrier layer, and a base electrode layer and emits or radiates plane waves of hot electrons by means of the tunnel effect when bias is applied between the emitter and base electrodes. A fraction of the emitted electrons maintains their energy and phase until they reach the end of the propagation layer. In the propagation space, these electrons or waves construct quantum mechanical

 © 2003 The American Physical Society

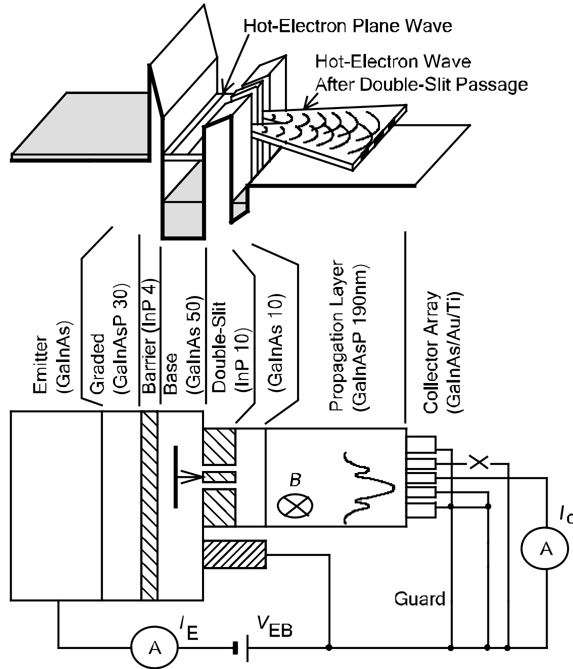

FIG. 1. Band profile and cross section of the device and measurement circuit for the double-slit interference observation of ballistic hot electrons. The interference pattern is conceptually drawn in the cross section. In the completed device, only the central collector was intact. The upper collector was unintentionally disconnected, while the lower collector had a leakage path to the guard electrode.

interference fringes owing to the double slit. A magnetic field B sweeps these interference fringes over the collector array. Then the collector current is modulated to enable us to observe the double-slit interference. In the base and the propagation layers, the electron state is three dimensional and far from equilibrium. The interference caused by the double slit takes place in the propagation layer consisting of the intrinsic semiconductor, where the electron energy is higher than the conduction-band bottom by more than 50 meV and the Fermi energy is in the midgap in contrast with 2DEG experiments.

A set of parameter values which enable the observation of the double-slit interference is designed as follows. The hot-electron energy is 0.1 eV and consequently, the wavelength is 20 nm in the GaInAsP propagation layer. The propagation layer thickness L is 200 nm which is equal to or less than the phase coherent length [22,23]. When the collector array pitch T and the center-to-center space d of the double slit satisfy $Td \leq 2000$ nm^2, high-contrast fringes are observable. To meet this essential requirement, state-of-the-art nanofabrication technologies are employed. Because of the limited coherent length of the ballistic hot electron in semiconductors, this requirement is much more severe than that for 2DEG interference observation. A 25-nm-space double slit [19] and a 80-nm-pitch collector array [21] enable us to distinguish the weak interference pattern. In addition, the transverse coherence determined by the emitter structure must be sufficiently high. The Fermi energy in the emitter electrode E_F is 6 meV so that E_F (meV) $\leq 8000/d^2$(nm^2) [24]. A graded layer where x and y in $Ga_xIn_{1-x}As_yP_{1-y}$ are gradually varied is inserted to prevent the electron accumulation adjacent to the barrier under V_{EB} application, which degrades the transverse coherence [24]. The tunnel barrier thickness is as small as 4 nm to allow high current density. Resistances between proximately neighboring collectors are higher than 10 MΩ [21] owing to the potential step between the propagation layer and the collector and the removal of conductive layers from between electrodes. Guard electrodes are arranged to prevent leakage current flow into the collectors.

The device fabrication process is as follows. On InP substrates, the layers up to the GaInAs layer on the double-slit InP layer (Fig. 1) were grown by metal organic vapor phase epitaxy (MOVPE). n-GaInAs (thickness of 400 nm and doping concentration of 2×10^{16} cm^{-3}), graded n-GaInAsP (30 nm, 2×10^{16} cm^{-3}), i-InP (4 nm), i-GaInAs (2.6 nm), n-GaInAs (44.8 nm, 2×10^{17} cm^{-3}), i-GaInAs (2.6 nm), i-InP (10 nm), and thin i-GaInAs were sequentially grown. The thin GaInAs layer functioned as an etching mask for transferring a double-slit pattern to the InP layer by wet-chemical etching [25]. Using electron-beam exposure (EBX) [19], two parallel slits with 12 nm openings, center-to-center distance of 25 nm, and length of 2 μm were fabricated. The double slit was buried within GaInAs and the remaining i-GaInAs (10 nm), i-GaInAsP (180 nm), i-GaInAs (10 nm), and n-GaInAs (15 nm, 5×10^{18} cm^{-3}) layers were sequentially grown by MOVPE. The base mesa of 16×15 μm^2 and the collector mesa of 4×8 μm^2 were formed. Base electrodes were formed by evaporating 20/230-nm-thick Cr/Au. On the top of the collector mesa, aligned with the double slit, seven electrodes with 4 μm length and 80 nm pitch were formed by EBX and the lift-off technique after an evaporation of 10/20-nm-thick Ti/Au. The collectors were separated by reactive ion etching. The entire surface was covered once with benzocyclobutene and then windows were opened for internal connection pads. Collectors of 40 nm width were connected to the wire-bonding pads via two-step wirings. EBX and photolithography were applied 11 and 3 times, respectively, to complete the devices.

In the completed device, the upper collector was unintentionally disconnected, while the lower collector had a leakage path to the guard electrode (see Fig. 1). Consequently, the collector current was measured accurately only for the central collector. Emitter and collector current-voltage characteristics at $T = 4.2$ K and $B = 0$ are shown in Fig. 2. The emitter current I_E comprised an intrinsic tunnel current I_e and an Ohmic current. I_e was extracted by eliminating the linear component, as shown by open circles in Fig. 2. The solid line is the theoretical tunnel current where the height of the triangular potential barrier of the graded layer and the effective

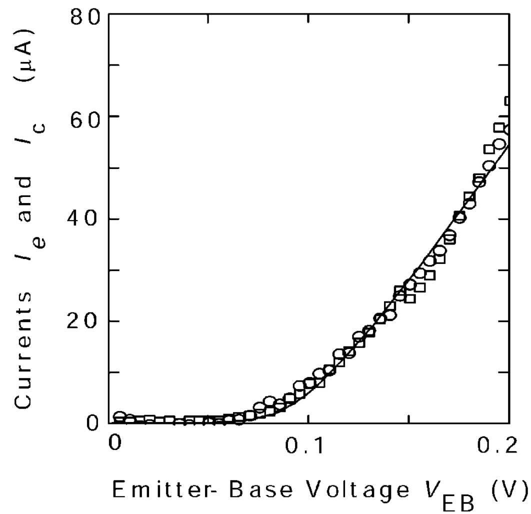

FIG. 2. Tunnel emission and collector currents versus emitter-base voltage at 4.2 K and $B = 0$. Open circles are the tunnel emission current I_e derived from the measured emitter current by subtracting the Ohmic component. Open squares are the collector current I_c multiplied by 3×10^5. The solid line is the theoretical tunnel current.

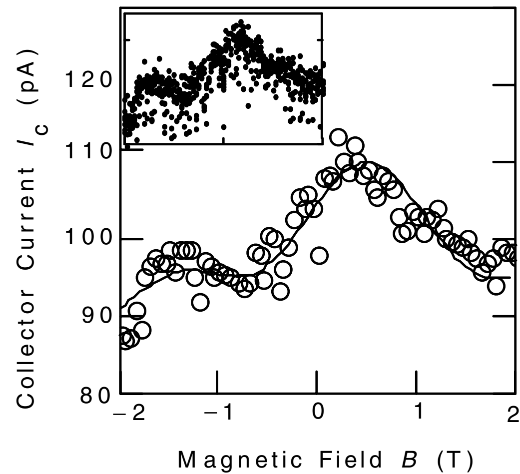

FIG. 3. Collector current versus magnetic field measured at 4.2 K and $V_{EB} = 0.16$ V. Open circles are medians of recorded data while the inset shows all data. The solid line is a theoretical curve.

base resistances were chosen to be 80 meV, which is close to the design value of 100 meV, and 1.1 kΩ, to achieve a good fit. The tunnel current coincides well with the theory. Furthermore the collector current multiplied by 3×10^5 coincides well with I_e. This coincidence implies that the electrons passing through the emitter barrier, the base layer, the double-slit opening, and the propagation layer carried the collector current.

Keeping V_{EB} at 160 mV, the collector current was measured and recorded 7 times for each value of B. In Fig. 3, each open circle shows the median of each group of seven values, while the inset shows all data. During the measurement, the emitter and the base currents were constant within 0.7% and 0.5%, respectively. On the basis of measurements of resistances between terminals, the voltage V_{EB} between the external emitter and the external base terminals was divided into two parts. Half the V_{EB} of 80 mV was applied across the emitter tunnel barrier while the other 80 mV was applied across the base contact resistance. Therefore, 80 mV was applied across the propagation layer. The interference pattern and consequent modulation in the collector current were simulated using the quantum beam propagation method [26], as shown by the solid line in Fig. 3. Disconnection in one neighboring collector was taken into account by increasing the collection range from 80 to 120 nm. Misalignments at the centers of the collector and the double slit, as well as the interference contrast, were adjusted to achieve a good fit. The misalignment was estimated to be 40 nm. The measured modulation coincides well with the theory.

During the observation, the tunnel emission current I_e was 30 μA, the component of the collector current I_{coh} modulated by the interference was 23 pA, and the constant component I_{incoh} was 100 pA (Figs. 2 and 3). The ratio η of the number of electrons entering into the propagation layer to that of all emitted electrons is the product of two transmission coefficients, one at the double slit and the other at the potential step behind it. The former is 2×10^{-4} (=double-slit opening area/total emitter area). The latter is of the order of 1 [27]. Therefore, 6 nA ($= \eta I_e$) passed through the double-slit openings. Since electrons are scattered, except for a small fraction in the base and propagation layers, an approximately uniform distribution over the end plane of the propagation layer is assumed. Then the estimated collector current becomes 180 pA (=6 nA × collection range/collector mesa width), which is in agreement with I_{incoh} in the order of magnitude.

Total interference current is 1.9 times the peak value of I_{coh}, 23 pA, according to the simulation, which is 43 pA. The ratio of this to ηI_e, 0.007, corresponds to the proportion of the coherent interfering electron or the probability of coherent transmission. As shown in Fig. 1, the electron emitted from the emitter passes through the base layer, the double-slit opening, the intermediate layer, and the propagation layer, sequentially. The electron concentration is of the order of 10^{17} cm^{-3} in the base and the intermediate layers, while it is 10^{15} cm^{-3} in the propagation layer. In the base and the intermediate layers, the electron-electron scattering determines the phase coherent length and is estimated to be 27 nm for the electron with the excess energy of 80 meV, measured from the Fermi energy at 4.2 K, estimated according to the literature [23]. In the propagation layer, spontaneous emission of the LO phonon determines the phase coherent length and is estimated as 130 nm using the scattering time of 0.2 ps [13,23] for a kinetic energy of 50 meV. Estimated inelastic scattering probabilities are 0.93

through the base, double-slit, and intermediate layers, and 0.77 in the propagation layer. Then the probability at which the electron arrives at the collector without any scattering is 0.016(= (1–0.93)(1–0.77)). The above-estimated experimental proportion of the coherent interfering electron, 0.007, coincides with this estimation in order of magnitude.

The incident electron on the slit was collimated within $\pm 12°(=\sqrt{6/135}$ rad). The excitation of the first higher mode by the collimated hot electron is 0.011 times that of the fundamental mode. Therefore, the passage through the slit is substantially limited to a single mode.

The present observation indicates that the wave front spread of the hot electron is more than the double-slit space of 25 nm and is consistent with the theoretical value of the wave front spread of 60 nm [28].

On the basis of critical inspections of the measured data, we believe that Young's double-slit interference of the hot electron in man-made semiconductor structures has been observed. This achievement may open the door to the creation of novel devices with sophisticated functions provided by electrons.

The authors thank S. Arai, M. Asada, and M. Watanabe for discussions and S. Tamura for support with EBX. This work is based on research accumulation of the last ten years. During those years, M. Suhara, H. Hongo, M. Gault, J. Suzuki, H. Tanaka, T. Hattori, A. Kokubo, H. Oguchi, H. Nakamura, and Y. Shirai contributed to the research. Y. Iye, University of Tokyo, supported us at the start-up of our measurements. This project was supported by Grants-in-Aids for Scientific Research from MEXT, Japan, including the interuniversity research program "Quantum Coherent Electronics: Physics and Technology."

*Electronic address: furuya@pe.titech.ac.jp

[1] L. Esaki and R. Tsu, IBM J. Res. Dev. **14**, 61 (1970).
[2] *Mesoscopic Physics and Electronics*, NanoScience and Technology, edited by T. Ando *et al.* (Springer, Berlin, 1997).
[3] A. Yacoby, U. Sivan, C. P. Umbach, and J. M. Hong, Phys. Rev. Lett. **66**, 1938 (1991).
[4] R. Crook *et al.*, J. Phys. Condens. Matter **12**, L167 (2000).
[5] M. A. Topinka *et al.*, Nature (London) **410**, 183 (2001).
[6] T. J. Thornton *et al.*, Phys. Rev. Lett. **56**, 1198 (1986).
[7] L.W. Molenkamp *et al.*, Phys. Rev. B **41**, 1274 (1990).
[8] J. J. Koonen, H. Buhmann, and L.W. Molenkamp, Phys. Rev. Lett. **84**, 2473 (2000).
[9] M. Heiblum, Solid-State Electron. **24**, 343 (1981).
[10] N. Yokoyama *et al.*, Jpn. J. Appl. Phys. **23**, L311 (1984).
[11] T. Ishibashi and Y. Yamauchi, IEEE Trans. Electron Devices **35**, 401 (1988).
[12] D. Rakoczy, G. Strasser, and J. Smolinera, Appl. Phys. Lett. **81**, 4964 (2002).
[13] D. Sicault *et al.*, Phys. Rev. B **65**, 121301 (2002).
[14] M. Kast *et al.*, Phys. Rev. Lett. **89**, 136803 (2002).
[15] K. Furuya, J. Appl. Phys. **62**, 1492 (1987); J. Cryst. Growth **98**, 234 (1989); Jpn. J. Appl. Phys. **30**, L82 (1991).
[16] A. Tonomura *et al.*, Phys. Rev. Lett. **48**, 1443 (1982).
[17] H. Hongo *et al.*, Jpn. J. Appl. Phys. **33**, 925 (1994).
[18] H. Hongo, Y. Miyamoto, M. Suhara, and K. Furuya, Appl. Phys. Lett. **70**, 93 (1997).
[19] Y. Miyamoto *et al.*, J. Vac. Sci. Technol. B **16**, 3894 (1998).
[20] Y. Miyamoto *et al.*, Appl. Surf. Sci. **159–160**, 179 (2000).
[21] Y. Miyamoto *et al.*, in *Proceedings of the Indium Phosphide and Related Materials Conference, Stockholm, Sweden, 2002* (IEEE, Piscataway, NJ, 2002), p. 585.
[22] A. F. J. Levi, J. R. Hayes, P. M. Platzman, and W. Wiegmann, Physica (Amsterdam) **134B**, 480 (1985).
[23] B. Y. K. Hu and S. Das Sarma, Semicond. Sci. Technol. B **305**, 7 (1992).
[24] H. Hongo, Y. Miyamoto, M. Gault, and K. Furuya, J. Appl. Phys. **82**, 3846 (1997).
[25] E. Inamura *et al.*, Jpn. J. Appl. Phys. **28**, 2193 (1989).
[26] N. Machida, H. Tamura, and K. Furuya, in *Springer Proceedings in Physics*, edited by N. Miura and T. Ando (Springer, Berlin, 2001), Vol. 87, p. 1723.
[27] K. Imamura *et al.*, Electron. Lett. **22**, 1148 (1986).
[28] H. Matsuura and K. Furuya, Jpn. J. Appl. Phys. **34**, 3589 (1995).